

A dissolved oxygen sensor based on composite fluorinated xerogel doped with platinum porphyrin dye

Yun Zhao^a, Tingxiu Ye^c, Haixu Chen^a, Dapeng Huang^c, Tingyao Zhou^a, Chunyan He^c and Xi Chen^{a,b,*}

ABSTRACT: A new functional fluorinated material taking *n*-propyltrimethoxysilane (*n*-propyl-TriMOS) and 3,3,3-trifluoropropyltrimethoxysilane (TFP-TriMOS) as precursors was applied to construct a novel dissolved oxygen sensing film. The sensing film was fabricated by dip-coating the functional fluorinated material-doped [meso-tetrakis(pentafluorophenyl) porphyrinato] platinum(II) (PtF₂₀TPP) onto a glass slide. The oxygen sensing film exhibited a good linear relationship, fast response time, long stability and high sensitivity to dissolved oxygen. In the developed optical oxygen sensor, an LED and a photodiode were composed to construct a back-detection optical system not needing an optical fiber based on fluorescence intensity detection. The smart optical oxygen sensor based on the PtF₂₀TPP fluorescence quenching possesses the advantages of portability and low cost and can be applied to the dissolved oxygen *in situ* monitoring in seawater. Copyright © 2009 John Wiley & Sons, Ltd.

Keywords: dissolved oxygen sensor; optical; fluorinated xerogels; platinum porphyrin dye; fluorescence quenching

Introduction

Nowadays, dissolved oxygen (DO) sensors have extensive applications in oceanography, meteorology, biology, environmental science and life science. Considerable efforts have been devoted to the development of optical dissolved oxygen sensors. Compared with electrochemical oxygen sensors, the optical dissolved oxygen sensors have great advantages, such as no oxygen consumption in the sensing process, no requirement for the reference electrode, inertness against sample flow rate or stirring speed and immunity to exterior electromagnetic interference. (1) In general, optimizing the performance of an optical oxygen sensor consists of three parts: the use of dyes with long unquenched state lifetime; the use of matrices with high oxygen permeability; and accurate determination methods. Among the oxygen probes, platinum porphyrin complexes are generally efficient luminophors (2–4) since they show strong phosphorescence at room temperature, visible light excitation and large Stoke's shift. (2) Moreover, their longer excited-state time of up to microseconds is the key reason for their being good candidates as optical oxygen probes. (5) In this work, we selected [meso-tetrakis (pentafluorophenyl) porphyrinato] platinum(II) (PtF₂₀TPP) as a fluorescent probe for the determination of dissolved oxygen.

The supporting material implemented to embed the oxygen probe plays a vital role in the fabrication of a dissolved oxygen sensor since the material greatly affects the characteristics of the sensing film. Unlike determination of gaseous oxygen, an efficient host matrix of the dissolved oxygen sensor must be highly permeable to oxygen but impermeable to liquid

water, heavy metal ions and other co-existing substances. The organically modified silicates (ORMOSILs) matrix has been widely used for oxygen sensors since it has high oxygen permeability, good mechanical and chemical stability and superior optical clarity. (6–9) Nowadays, new functional fluorinated materials have attracted great attention due to their enhanced hydrophobicity, high thermal and oxidative stability, weak intermolecular interactions, low light absorption, exceptional chemical and biological inertness, and high gas-dissolving capacity. In addition, fluorinated ORMOSILs, in particular, exhibit a number of extraordinary properties such as greatly enhanced thermal and chemical stability and higher hydrophobicity imparted by fluorine to these organic–inorganic composites. (10) Nowadays, besides

* Correspondence to: X. Chen, Department of Chemistry and Key Laboratory of Analytical Sciences of the Ministry of Education, College of Chemistry and Chemical Engineering, Xiamen University, Xiamen 361005, People's Republic of China. E-mail: xichen@xmu.edu.cn

^a Department of Chemistry and Key Laboratory of Analytical Sciences of the Ministry of Education, College of Chemistry and Chemical Engineering, Xiamen University, Xiamen 361005, People's Republic of China

^b State Key Laboratory of Marine Environmental Science, Xiamen University, Xiamen 361005, People's Republic of China

^c Ministry of Education Key Laboratory of Analysis and Detection Technology for Food Safety, Fuzhou University, Fuzhou 350002, People's Republic of China

ORMOSILs, utilization of fluorinated ORMOSILs has been well developed. (2,11–13) Bukowski *et al.* (13) developed a highly sensitive gaseous sensor composed of *n*-propyltrimethoxysilane (*n*-propyl-TriMOS) and 3,3,3-trifluoropropyltrimethoxysilane (TFP-TriMOS) taking tris(4,7-diphenyl-1,10-phenanthroline) ruthenium(II) ([Ru(dpp)₃]²⁺) as a luminophore. Chu *et al.* (2) fabricated two kinds of high-performance quenchometric fiber-optic sensors for gaseous oxygen based on *n*-propyl-TriMOS/TFP-TriMOS doped with platinum complexes. These sensors exhibited better sensitive performance and shorter response time than those using [Ru(dpp)₃]²⁺ in various sol–gel matrixes.

Generally, there are two basic modes for optically monitoring dissolved oxygen concentration: fluorescence intensity method (7,8,14–20) and fluorescence lifetime measurement. (21–25) The former mode is still a very common measuring mode due to its simplicity and low cost. The major disadvantages of the fluorescence intensity measurement include susceptibility to light source and detector drift and degradation or leaching of the dye. (26) These drawbacks could be effectively avoided by calibration before the determination, using photochemically stable probes and choosing good performance sensing film. Fluorescence lifetime is an intrinsic important parameter of fluorophore and independent of perturbation of excitation intensity, detector sensitivity and drift, photo decomposition and indicator concentration. (27) However, the fluorescence lifetime measurement requires sophisticated instruments. Nowadays, most dissolved oxygen sensors need expensive quartz optical fibers for transmitting light, which increases the equipments for determination *in situ*. Moreover, some oxygen sensors use a fluorimeter or CCD as the detector and traditional 90° optical design for the light source and detector, which does not in favor of the miniaturization and low cost of the dissolved oxygen sensor. In this study, we developed a novel optical oxygen sensor using a uniform and crack-free oxygen sensing film composed of *n*-propyl-TriMOS/TFP-TriMOS doped with PtF₂₀TPP. In the smart optical oxygen sensor, an LED and a photodiode were composed to construct a back-detection optical system not needing an optical fiber based on fluorescence intensity detection. The dissolved oxygen sensor possesses the advantages of portability, low cost and shows a very good linearity of the concentration of dissolved oxygen up to 15.50 mg L⁻¹ by fitting a multi-site model²⁸ of the modified Stern–Volmer equation. The oxygen sensor was applied to the *in situ* detection of dissolved oxygen in seawater. Satisfactory results were obtained when its analytical performance was compared with a typical Clark-type oxygen electrode.

Experimental

Chemicals

Platinum complex, [meso-tetrakis (pentafluorophenyl) porphyrinato] platinum(II) (PtF₂₀TPP), used as an oxygen sensitive indicator was synthesized and purified as described in the literature. (5) *n*-Propyl-TriMOS and Triton X-100 were from Sigma Aldrich (St Louis, MO, USA). TFP-TriMOS was purchased from Alfa Aesar (Germany). All other chemicals used in this study were analytical reagent grade and all solutions were prepared with deionized distilled water. Nitrogen and oxygen gases (99.9%) were purchased from Xiamen Oxygen Manufactory (Xiamen, China).

Apparatus

Absorption spectra of the sensing film were measured using a Evolution 300 UV–vis spectrophotometer (Thermo, USA). Fluorescence profiles of the oxygen sensor were obtained from F-4500 spectrofluorimeter (Hitachi, Japan). A scanning electron microscope (SEM) (LEO1530, Leo, Germany) was used to obtain the scanning electron micrograph of the oxygen-sensing film. Two sets of CMOsens SFC 4000 mass flow controllers (Sensirion AG, Switzerland), which can be accurately controlled by a CMOsens EM1 intelligent flowmeter, were utilized to control the relative flow rates of oxygen and nitrogen gases. Samples with different dissolved oxygen concentration were prepared by flowing the mixtures of oxygen and nitrogen gases into a sealed cell of deionized water. The dissolved oxygen samples were calibrated by a Dissolved Oxygen Meter Model YSI5000 (Yellow Springs Instrument Co. Inc., USA). The performance of our developed optical oxygen sensor was compared with a commercial dissolved oxygen meter model YSI6562 (Yellow Springs Instrument Co. Inc., USA) in seawater. All measurements were performed under an air-conditioned environment having a constant temperature of 20 ± 1°C. Different temperatures were controlled by a Julabo F12-ED refrigerated/heating circulator (Julabo Inc., Germany) for the investigation of the temperature effect.

Oxygen sensing film preparation

A 0.69 mL aliquot of *n*-propyl-TriMOS and 1.5 mL of TFP-TriMOS were placed in an open vial. Then, 1.5 mL EtOH and 0.08 mL HCl (0.1 M) were added to the mixture to catalyze the ORMOSILs reaction. The solution was capped and stirred magnetically for 1 h at room temperature. During the stirring process, 0.1 mL Triton X-100 was added to the solution, resulting in a crack-free monolith. (2,13) The luminophore-doped sol solutions were prepared by dissolving 2 mg mL⁻¹ PtF₂₀TPP–THF solutions into the sol solution and vigorously stirred for 10 min to ensure homogenization. Films were prepared by pipetting 15 µL of the mixture onto a glass slide (25 × 12.5 mm²) which had been soaked in NaOH (0.1 M) for 24 h and washed with distilled water and ethanol. The resulting films were cured for 24 h at room temperature. According to measurements using SEM, the thickness of the films prepared in this way was estimated to be 5.6 µm (Fig. 1), which not only guarantees a higher fluorescence intensity change but also decreases the response time of the oxygen sensor because of the relatively thin thickness.

Construction of the optical dissolved oxygen sensor

The sensor setup is shown in Fig. 2. An LED with the maximum wavelength of 390 nm (light-emitting angle <15° and half-band width <20 nm) was selected as the excitation source, and directed to the oxygen sensing film. To improve the light stability of the LED, constant electric current was selected to be a power supply. A silicon photodiode (Burr-Brown, OPT301) with a transimpedance amplifier, which converts the fluorescence signal detected into the electric signal, was employed. In the optical sensor, the central axes of the LED and the photodiode were kept parallel. Comparing to the ordinary vertical mode between the light source and the detector unit, this design minimized the sensor volume, and kept the total volume $\pi \times 26^2 (R^2) \times 80 (H) \text{ mm}^3$. An optical band-pass filter (645 ± 15 nm) was used to separate the excitation light from the emission.

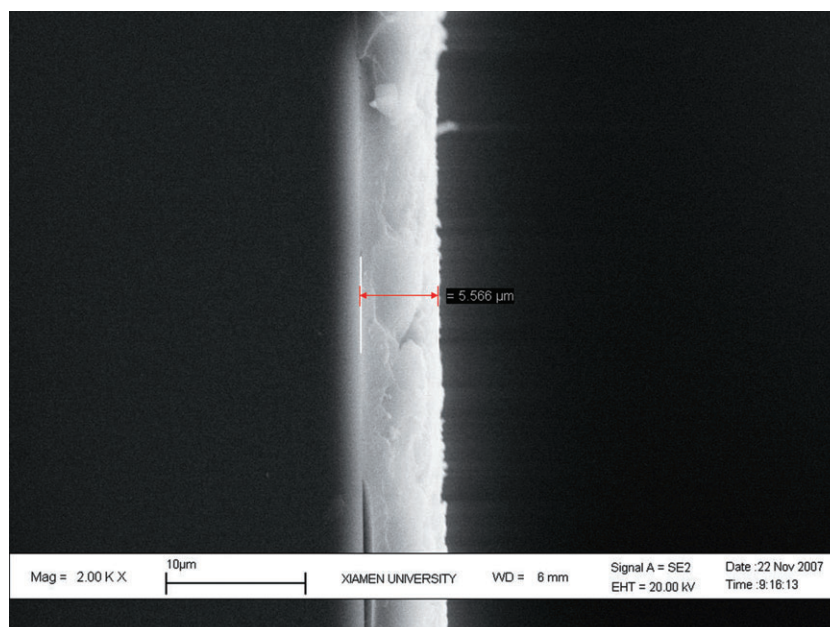
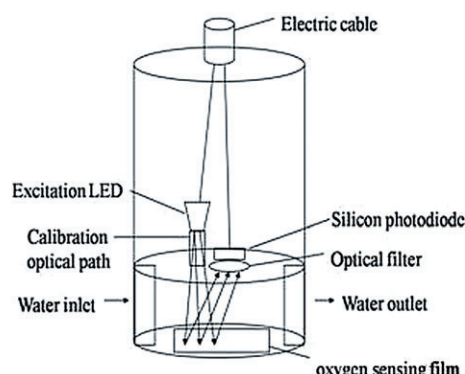


Figure 1. Scanning electron micrograph of oxygen sensing film.



(a)



(b)

Figure 2. Diagrams of the dissolved oxygen sensor: the physical view of the sensor (a) and the design view of the sensor (b).

Results and discussion

Spectroscopic behavior of the oxygen-sensitive film

The visible absorption of PtF₂₀TPP is mainly $\pi \rightarrow \pi^*$ and largely porphyrin-centered. The heavy metal ion facilitates intersystem crossing to the triplet state, which has a significantly longer τ_0 and enhances oxygen quenching. Meanwhile, the atomic number of platinum enhances spin-orbit coupling so that the triplet state τ_0 is not so long as to be totally quenched by environmental interactions or trace quenchers. As shown in Fig. 3, the absorption feature of PtF₂₀TPP entrapped in the fluorinated ORMOSILs film remains almost the same as that dissolved in THF solution, indicating that there is no interaction between PtF₂₀TPP and the fluorinated ORMOSILs film. It can be found that the PtF₂₀TPP xerogel has a Soret band at 389 nm and two Q bands of 505 nm

and 538 nm. In this case, we selected the LED with a maximum wavelength of 390 nm as the excitation light source for the dissolved oxygen sensor. The luminescence excitation and emission spectra of the oxygen sensing film doped with PtF₂₀TPP in pure nitrogen are shown in Fig. 4. It can be found that PtF₂₀TPP-doped oxygen sensor exhibited strong luminescence emission at 645 nm in pure nitrogen environment. The large Stokes shift about 255 nm effectively avoids the interference of the excitation light source with the luminescence emission detection.

Dissolved oxygen sensing

The quenching of the oxygen sensing probe, which obeys the rule of the Stern–Volmer (SV) equation, is generally applied in the optical sensing determination of oxygen. The SV equation

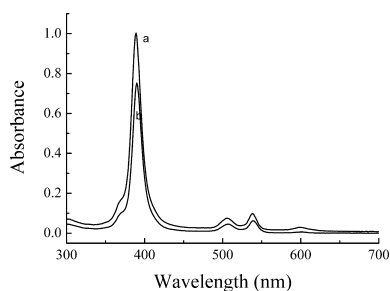


Figure 3. Comparison of absorption spectra of PtF₂₀TPP dissolved in THF solution (a) and that within the fluorinated ORMOSILS matrix (b).

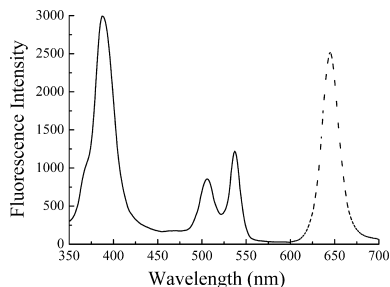


Figure 4. Excitation and emission spectra of PtF₂₀TPP-doped oxygen sensor in pure gaseous nitrogen environment.

quantitatively relates lifetime and luminescence intensity to oxygen concentration [eqn (1)]:

$$\frac{l_0}{l} = \frac{\tau_0}{\tau} = 1 + K_{sv} [O_2] \quad (1)$$

where K_{sv} is the SV quenching constant; τ and τ_0 are the quenched and unquenched fluorescence lifetimes, respectively; l and l_0 are the quenched and unquenched fluorescence intensities, respectively. The response of an ideal sensor based on SV kinetics quenching has a linear relationship towards O_2 concentration. In a solid matrix, non-linear SV plots are often obtained attributed to an inhomogeneous dye distribution in the matrix.

In the oxygen sensor, with the increase of the oxygen concentration, the luminescence intensity of PtF₂₀TPP decreased. The sensor quenching response over a range of dissolved oxygen concentration is shown as a Stern–Volmer plot in Fig. 5. The plot exhibited downward turning at higher oxygen concentrations, indicating that the dye molecules reside in different sites in the matrix with different accessibility to the quencher oxygen, which is attributed to the dynamic quenching theory. (28) Assuming a distribution of dye molecules with varying sensitivity to dissolved oxygen quencher, the SV equation can be written as eqn (2): (28)

$$\frac{l_0}{l_0 - l} = \left\{ \sum \frac{f_i K_{svi} [O_2]}{1 + K_{svi} [O_2]} \right\}^{-1} \quad (2)$$

where f_i is the fraction of dye molecules i with a quenching constant K_{svi} .

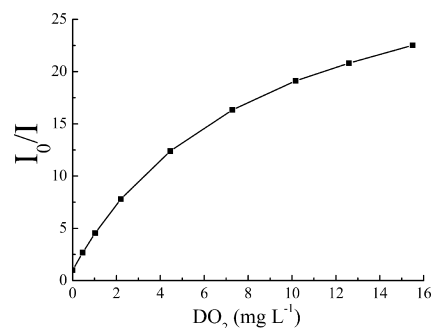


Figure 5. Stern–Volmer plot for PtF₂₀TPP in fluorinated ORMOSILS matrix.

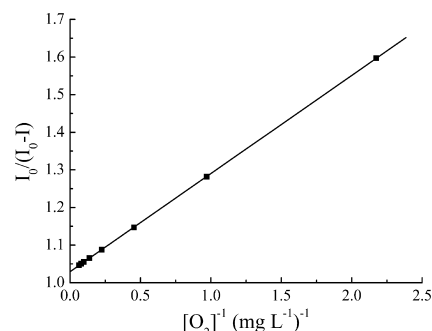


Figure 6. Modified multi-site Stern–Volmer plot for PtF₂₀TPP in the oxygen sensing film.

This equation can be written as shown in eqn (3):

$$\frac{l_0}{l_0 - l} = \frac{1}{fK_{sv}[O_2]} + \frac{1}{f} \quad (3)$$

where $f = \sum f_i$ is the maximum mole fraction of dye molecules which are quenched by oxygen. If all chromophore molecules are quenched to the same degree, $f = 1$. According to this modified SV equation, a plot of $l_0/(l_0 - l)$ against $1/[O_2]$ based on the data, as shown in Fig. 5, could be constructed, and the result is shown in Fig. 6. The linear relationship can be described by eqn (4):

$$y = 1.03 + 0.26x \quad (4)$$

where $y = l_0/(l_0 - l)$ and $x = 1/[O_2]$. In this equation, an intercept of $1/f = 1.03$ and $R^2 = 1.0000$ with a linearity up to the dissolved oxygen concentration of 15.50 mg L^{-1} could be found. The detection limit of the oxygen sensor was 0.01 mg L^{-1} . The good linearity over a large concentration range facilitates the calibration of the oxygen sensor in practical applications.

Response performance, photostability and storage stability of the fluorinated ORMOSILs film

The typical dynamic recovery response experiment (29) of the PtF₂₀TPP-doped sensing film indicated that stable and reproducible signals could be obtained. The fluorescence quenching rate (l_0/l_{100}) from nitrogen-saturated (l_0) to oxygen-saturated (l_{100}) solution was up to 78, and the response time was 4 s from nitrogen-saturated to oxygen-saturated state and 263 s for the reverse case. (29) These results show a very high sensitivity, good repro-

Table 1. Results of dissolved oxygen determination of seawater samples in Xiamen^a ($n = 5$)

| Sample no. | Sampling pot | Proposed method (mg L ⁻¹) | Electrochemical probe method (mg L ⁻¹) | Relative error (%) |
|------------|-------------------------|---------------------------------------|--|--------------------|
| 1 | N24°26.652'E118°09.333' | 8.75 ± 0.06 | 8.44 ± 0.05 | 3.67 |
| 2 | N24°25.841'E118°06.620' | 8.96 ± 0.07 | 8.64 ± 0.03 | 3.70 |
| 3 | N24°25.819'E118°06.057' | 8.79 ± 0.04 | 8.71 ± 0.02 | 0.92 |
| 4 | N24°26.089'E118°05.875' | 7.85 ± 0.10 | 7.60 ± 0.06 | 3.29 |
| 5 | N24°24.363'E118°06.682' | 8.43 ± 0.11 | 8.79 ± 0.05 | -4.10 |

^aRefluent seawater, sunshiny, sampling date, 20 April 2009.

ducibility and fast response time to dissolved oxygen because of the considerably higher oxygen diffusivity within these hybrid xerogels. The photostability of the PtF₂₀TPP-doped sensing film was also tested by exposing it under the light irradiation of 390 nm for 10 h. Less than a 2% decrease of the fluorescence intensity could be found. This photostability of PtF₂₀TPP is due to its four fluorophenyl groups attaching to the porphyrin. The long-term quenching stability was investigated by measuring the overall quenching response value I_0/I_{100} as a function of time. No significant change could be observed over a 6 month storage in the dark. Because of the high hydrophobic properties of the sensing film, there was no detectable luminescence in water after the film was stored in it for six months.

Effect of measurement temperature

Since oxygen sensors are prone to the influence of temperature, the effect of temperature on the oxygen sensing film was investigated in nitrogen-saturated water. The temperature range from 5 to 40°C with an interval of 5°C was selected. A 45.5% decrease of fluorescence intensity of the PtF₂₀TPP-doped oxygen sensor was found when the measurement temperature was changed from 5 to 40°C. This result reveals that the calibration under different temperature is necessary in the determination of dissolved oxygen. In the practical application, the temperature calibration could be implemented by constructing the different linear plots of $I_0/(I_0 - I)$ against $1/[O_2]$, by a two-point method when the temperature was changed from 5 to 40°C with an interval of 5°C. In our experiment, all measurements were performed under a constant temperature of $20 \pm 1^\circ\text{C}$.

Salinity effect of the sensing response

In the application of oxygen determination in seawater, the effect of salinity on the oxygen sensing response should be taken into account. The experimental results revealed that a less than 4% change of I_0/I_{100} could be found when the sample salinity ranged from 5 to 40‰. Because the salinity of seawater in the general case is about 35‰, the effect of salinity on the oxygen sensing response could be ignored in practical applications. The excellent anti-salinity of the sensing film could be attributed to its high hydrophobicity, which prevents the penetration of co-existing ions into the sensor matrix and facilitates application in seawater.

Application for dissolved oxygen determination of seawater

The optical dissolved oxygen sensor was applied to determine the dissolved oxygen concentrations of seawater in the Xiamen

area of Fujian, China. The results were compared with the national standard method of China (GB 11913-89) using a commercial dissolved oxygen meter model YSI6562. As shown in Table 1, there was no obvious difference between the proposed method and the GB 11913-89 method. The relative errors of all determination results were less than 5%, indicating that the developed optical sensor presented excellent performance in the detection of dissolved oxygen in seawater.

Conclusions

A novel dissolved oxygen sensor was fabricated with fluorinated ORMOSILS *n*-propyl-TriMOS and TFP-TriMOS doped with platinum porphyrin complex PtF₂₀TPP. The film exhibited a good linear relationship, fast response time, long stability and high sensitivity to dissolved oxygen due to the excellent characteristics of the new functional fluorinated materials. The back-detection optical design of the smart dissolved oxygen sensor coupled with the high-performance sensing film shows a good linearity up to 15.50 mg mL⁻¹ by fitting a multi-site model of the modified Stern–Volmer equation. Herein, we believe that the new-built dissolved oxygen sensor has a great potential in monitoring dissolved oxygen in an aggressive seawater environment.

Acknowledgment

This work was financially supported by the National Science and Technology Development Project (863 project no. 2006AA09Z160) and the National Natural Scientific Foundation of China (no. 20775064), which are gratefully acknowledged. We thank Professor Kwok-yin Wong, The Hong Kong Polytechnic University, for providing oxygen sensor probes.

References

- Choi MMF, Xiao D. Oxygen-sensitive reverse-phase optode membrane using silica gel-adsorbed ruthenium(II) complex embedded in gelatin film. *Anal Chim Acta* 1999;387:197–205.
- Chu CS, Lo YL. High-performance fiber-optic oxygen sensors based on fluorinated xerogels doped with Pt(II) complexes. *Sens Actuators B Chem* 2007;124:376–82.
- Kalyanasundaram K. *Photochemistry of Polypyridine and Porphyrin Complexes*. Academic Press: New York, 1992.
- Amao Y, Miyashita T, Okura I. Metalloporphyrins immobilized in styrene-trifluoroethylmethacrylate copolymer film as an optical oxygen sensing probe. *J Porphyrins Phthalocyanines* 2001;5: 433–8.

5. Che CM, Hou YJ, Chan MCW, Guo J, Liu Y, Wang Y. [meso-Tetrakis(pentafluorophenyl)porphyrinato]platinum(II) as an efficient, oxidation-resistant red phosphor: spectroscopic properties and applications in organic light-emitting diodes. *J Mater Chem* 2003;13:1362–6.
6. Lavin P, McDonagh CM, MacCraith BD. Optimization of Ormosil films for optical sensor applications. *J Sol–Gel Sci Technol* 1998;13:641–5.
7. McDonagh CM, MacCraith BD, McEvoy AK. Tailoring of Sol–Gel Films for Optical Sensing of Oxygen in Gas and Aqueous Phase. *Anal Chem* 1998;70:45–50.
8. Chen X, Zhong Z, Li Z, Jiang Y, Wang X, Wong K. Characterization of ormosil film for dissolved oxygen sensing. *Sens Actuators B Chem* 2002;87:233–8.
9. Pang HL, Kwok NY, Chow LMC, Yeung CH, Wong KY, Chen X, Wang X. ORMOSIL oxygen sensors on polystyrene microplate for dissolved oxygen measurement. *Sens Actuators B Chem* 2007;123:120–6.
10. Pagliaro M, Ciriminna R. New fluorinated functional materials. *J Mater Chem* 2005;15:4981–91.
11. Campostrini R, Ischia M, Garturan G, Armelao L. Sol–Gel Synthesis and Pyrolysis Study of Oxyfluoride Silica Gels. *J Sol–Gel Sci Technol* 2002;23:107–17.
12. Atkins GR, Charters RB. Optical properties of highly fluorinated and photosensitive organically-modified silica films for integrated optics. *J Sol–Gel Sci Technol* 2003;26:919–23.
13. Bukowski RM, Ciriminna R, Pagliaro M, Bright FV. High-performance quenchometric oxygen sensors based on fluorinated xerogels doped with [Ru(dpp)₃]²⁺. *Anal Chem* 2005;77:2670–2.
14. Carraway ER, Demas JN, DeGraaf BA, Bacon JR. Photophysics and photochemistry of oxygen sensors based on luminescent transition-metal complexes. *Anal Chem* 1991;63:337–42.
15. Trettnak W, Gruber W, Reininger F, Klimant I. Recent Progress in Optical Oxygen Sensor Instrumentation. *Sens Actuators B Chem* 1995;29:219–25.
16. McDonagh CM, Shields AM, McEvoy AK, MacCraith BD, Gouin JF. Optical sol-gel-based dissolved oxygen sensor: progress towards a commercial instrument. *J Sol–Gel Sci Technol* 1998;13:207–11.
17. McEvoy AK, McDonagh CM, MacCraith BD. Dissolved oxygen sensor based on fluorescence quenching of oxygen-sensitive ruthenium complexes immobilized in sol-gel-derived porous silica coatings. *Analyst* 1996;121:785–8.
18. Xiao D, Mo Y, Choi MMF. A hand-held optical sensor for dissolved oxygen measurement. *Meas Sci Technol* 2003;14:862–7.
19. Guo L, Ni Q, Li J, Zhang L, Lin X, Xie Z, Chen G. A novel sensor based on the porous plastic probe for determination of dissolved oxygen in seawater. *Talanta* 2008;74:1032–7.
20. Xiong X, Xiao D, Choi MMF. Dissolved oxygen sensor based on fluorescence quenching of oxygen-sensitive ruthenium complex immobilized on silica–Ni–P composite coating. *Sens Actuators B Chem* 2006;117:172–6.
21. McDonagh C, Kolle C, McEvoy AK, Dowling DL, Cafolla AA, Cullen SJ, MacCraith BD. Phase fluorometric dissolved oxygen sensor. *Sens Actuators B Chem* 2001;74:124–30.
22. Lakowicz JR. *Probe Design and Chemical Sensing. Topics in Fluorescence Spectroscopy. Vol 4* Plenum Press: New York, 1994.
23. Spichiger-Keller U. *Chemical Sensors and Biosensors for Medical and Biological Applications.* Wiley: New York, 1998.
24. Lippitsch ME, Kieslinger D, Draxler S. Luminescence lifetime-based sensing – new materials, new devices. *Sens Actuators B Chem* 1997;38:96–102.
25. Roche P, Al-Jowder R, Narayanaswamy R, Young J, Scully P. A novel luminescent lifetime-based optrode for the detection of gaseous and dissolved oxygen utilising a mixed ormosil matrix containing ruthenium (4,7-diphenyl-1,10-phenanthroline)₃Cl₂ (Ru.dpp). *Anal Bioanal Chem* 2006;386:1245–67.
26. Sánchez-Barragán I, Costa-Fernández JM, Valledor M, Campo JC, Sanz-Medel A. Room-temperature phosphorescence (RTP) for optical sensing. *TrAC Trends Anal Chem* 2006;25:958–67.
27. Morris KJ, Roach MS, Xu W, Demas JN, Degraff BA. Luminescence lifetime standards for the nanosecond to microsecond range and oxygen quenching of ruthenium(II) complexes. *Anal Chem* 2007;79:9310–4.
28. Gillanders RN, Tedford MC, Crilly PJ, Bailey RT. A composite thin film optical sensor for dissolved oxygen in contaminated aqueous environments. *Anal Chim Acta* 2005;545:189–94.
29. Zhao Y, Ye TX, Jiang YQ, Chen X, Wang XR. A composite fluorinated xerogels doped with platinum porphyrin dyes for dissolved oxygen sensing. *Luminescence* 2008;23:279–80.